Sensitization of the photoconductivity of conducting polymers by C_{60}: Photoinduced electron transfer

C. H. Lee, G. Yu, D. Moses, K. Pakbaz, C. Zhang, N. S. Sariciftci, A. J. Heeger, and F. Wudl
Institute for Polymers and Organic Solids, University of California, Santa Barbara, California 93106
(Received 10 June 1993)

We have investigated the effect of photoinduced electron transfer on the photoconductivity (PC) of conducting polymer-C_{60} films by comparing the photoconductivity (carrier generation and carrier transport) of the conducting polymer sensitized with C_{60} with that of the conducting polymer alone. We present time-resolved transient PC results, subnanosecond to 0.5 μs, obtained from poly[2-methoxy,5-(2'-ethyl-hexyloxy)-*p*-phenylene vinylene] (MEH-PPV) and poly(3-octylthiophene) (P3OT), and from conducting polymer films sensitized with several concentrations of C_{60}. Both the magnitude and the lifetime of the transient PC increase substantially on increasing the concentration of C_{60}. The results imply that quantum efficiency for photogeneration of charge carriers is increased by photoinduced electron transfer and that early time recombination is inhibited by the spatial separation of the electron and hole on the C_{60} and the conducting polymer, respectively. The greater enhancement of the transient PC in MEH-PPV (nearly two orders of magnitude with the addition of a few percent of C_{60}) than in P3OT (nearly one order of magnitude with the addition of a comparable amount of C_{60}) suggests a higher probability of early time recombination in pristine MEH-PPV. As a result of the enhancement in the photogeneration efficiency and the carrier lifetime, the spectral response of the steady-state PC in both MEH-PPV/C_{60} and P3OT/C_{60} films is significantly enhanced throughout the entire spectral range from the near infrared to the ultraviolet.

I. INTRODUCTION

Evidence for the photoinduced electron transfer from the excited state of poly [2-methoxy,5-(2'-ethyl-hexyloxy)-*p*-phenylene vinylene] (MEH-PPV) onto C_{60}, has been reported.[1,2] Photoinduced absorption (PIA) studies demonstrate a different excitation spectrum for the composite compared to that for the separate components, and the photoinduced electron resonance signal exhibits the spin-labeled signatures of both the conducting polymer cation and the C_{60} anion. The quenching of the photoluminescence of MEH-PPV by electron transfer onto C_{60} provided an estimate of the transfer rate ($>10^{12}$ s^{-1}) (Refs. 1 and 2) which was subsequently confirmed by direct time-resolved measurements.[3] The ultrafast charge transfer implies a high quantum efficiency; since charge transfer occurs nearly 10^3 times faster than any competing process, the quantum efficiency should be order unity. The implication of high quantum efficiency for charge transfer and charge separation stimulated the fabrication of donor-acceptor thin-film heterojunction diodes and photovoltaic cells.[4]

The C_{60} molecule is an acceptor capable of taking on as many as six electrons.[5-9] As a relatively good acceptor, C_{60} forms charge-transfer salts with alkali metals; these compounds are conductors[6] and exhibit superconductivity with relatively high temperatures.[7] Conducting polymers have relatively broad π (valence) and π^* (conduction) bands, and they can be doped over the full range from insulator to metal.[10,11] Although these materials are typically weak donors, semiconducting polymers can be synthesized with a range of ionization potentials and electron affinities by controlling the energy gap and electronegativity through molecular design and directed synthesis.[12,13]

Conducting polymers such as MEH-PPV and poly(3-octylthiophene) (P3OT) are sufficiently weak donors that charge transfer to C_{60} does not occur in the ground state; the conducting polymer and C_{60} form a neutral donor (D)-acceptor (A) complex. The optical absorption spectrum of the MEH-PPV/C_{60} composite is a simple superposition of the two components, implying relatively weak mixing of the ground-state electronic wave functions. For P3OT, a change in the absorption spectrum is observed upon adding C_{60}, indicating significant mixing of the P3OT and C_{60} ground-state electron wave functions with weak charge transfer in the ground state.[2,8] In neither case, however, is the ground state truly ionic (D^+-A^-).

After photoexcitation of the conducting polymer with photon energy greater than the π-π^* gap, electron transfer to the C_{60} molecule occurs in $<10^{-12}$ s.[1-3] The evolution from the photoexcited state of the D-A complex to free separated charge carriers is somewhat complex. Photoinduced charge transfer depends on the ionization potential (I_{D^*}) of the excited state of the donor, the electron affinity (A_A) of the acceptor, the Coulomb energy (U_C) of the separated ions (including polarization effects, i.e., dielectric relaxation of the molecular environment to stabilize the charge separation), and structural relaxation of the polymer backbone due to electron-lattice coupling. Photoinduced electron transfer cannot occur unless these quantities satisfy the following inequality $I_{D^*} - A_A - U_C < 0$. Charge separation can be

stabilized by carrier delocalization and by structural relaxation.

Free charge-carrier generation, facilitated by charge separation in the excited state, should result in significantly enhanced photoconductivity (PC). By inducing electron transfer from the photoexcited π^* band of the semiconducting polymer, the C_{60} serves to sensitize the photoconductive response. This sensitization should be particularly effective if the transfer rate is fast enough to be competitive with the mechanism(s) for early time recombination of photoexcited electrons and holes in the conducting polymer.

We have therefore, investigated the effect of photoinduced electron transfer on the photoconductivity of conducting polymer-C_{60} films by comparing the PC of the conducting polymer sensitized with C_{60} with that of the conducting polymer alone. Time-resolved transient PC results, subnanosecond to 0.5 μs, obtained from MEH-PPV and P3OT and from conducting polymer films sensitized with several concentrations of C_{60} demonstrate that both the magnitude and the lifetime of the transient PC increase substantially on increasing the concentration of C_{60}. Photoinduced electron transfer dramatically increases the quantum efficiency for photogeneration of charge carriers. Moreover, recombination is inhibited by the spatial separation of the electron and hole (on the C_{60} acceptor and on the conducting polymer donor, respectively). The enhancement of the transient PC is greater in MEH-PPV (nearly two orders of magnitudes with addition of a few percent of C_{60}) than in P3OT (nearly one order of magnitude with addition of a comparable amount of C_{60}) suggesting that the probability of early time recombination is higher in pristine MEH-PPV than in pristine P3OT. Because of the increased quantum yield and the increased carrier lifetime, the spectral response of the steady-state PC in both MEH-PPV/C_{60} and P3OT/C_{60} composites shows significantly enhanced PC from the near infrared to the ultraviolet, compared with that of the conducting polymer alone. The temperature dependence and light intensity dependence are investigated for both transient and steady-state PC to study the dynamics of charge carriers.

II. EXPERIMENTAL METHODS AND CHARACTERIZATION OF MEH-PPV/C_{60} AND P3OT/C_{60} FILMS

Thin films were prepared by drop casting or spincasting from solution onto alumina substrates for the photoconductivity measurement and onto glass substrates for the optical-absorption measurement. The synthesis and properties of MEH-PPV and P3OT have been described in earlier publications.[14,15] C_{60} powder was purchased in high purity (99.99%) from Polygon Enterprises.

The MEH-PPV/C_{60} mixture solutions (1,5, and 50% C_{60} solutions) were prepared by dissolving MEH-PPV and C_{60} in toluene in an appropriate weight ratio. The procedures for preparation of the P3OT/C_{60} mixture (5 wt % C_{60}) solutions have been described in detail previously.[2] The nominal C_{60} concentrations are specified as the wt % in the conducting polymer. The composite films are not as uniform as the films of the pure conducting polymer due to segregation of the less soluble C_{60} component.

Optical-absorption spectra were measured by transmission through thin films at room temperature using a Perkin Elmer Lambda 9 Spectrophotometer. Samples for the photoconductivity measurement were mounted onto the cold finger of a Helitran cryostat, and measurements were carried out in the temperature ranges from 300 to 81 K under a vacuum of less than 10^{-4} Torr.

The transient PC data were taken using the Auston microstripline-switch technique.[16] The microstripline gold electrodes were deposited on top of the sample (which was cast on an alumina substrate), leaving a gap of 200 μm between 600 μm-wide microstriplines. A gold backplane was deposited onto the back surface of the alumina substrate to form a transmission line with 50-Ω impedance and with a frequency response over 100 GHz. Details of the transient PC measurement using the Auston-switch transmission line configuration can be found in earlier publications.[17,18] One side of the microstrip was biased with 200 V, and the other side was connected to an EG&G PAR 4400 boxcar system fitted with a Tektronix S-4 sampling head. The boxcar was triggered with the light pulse via a photodiode. Excitation pulses were obtained from a PRA LN105A dye laser pumped with a PRA LN1000 N_2 laser operated at a repetition rate of 3–5 Hz. The pulse width was approximately 20–30 ps and the typical pulse intensity was about 2 μJ/pulse at $\hbar\omega = 2.92$ eV (425 nm). The overall temporal resolution of the detection system was about 50 ps, resulting from a combination of the gatewidth and trigger jitter of the boxcar system, the response of the cable transmission line between the probe and the boxcar, and the laser pulse width. For pristine MEH-PPV samples, however, the excitation pulse was the direct output from a PRA LN1000 N_2 laser at $\hbar\omega = 3.7$ eV (pulse width of approximately 600 ps) because the photocurrent of MEH-PPV is too small to measure using the lower intensity dye laser. The MEH-PPV data were obtained with a sampling gatewidth of 2 ns.

Data were obtained with uniform illumination of the sample across the 200-μm gap under the biasing electric field of 1×10^4 V/cm. To improve the signal-to-noise ratio, signal averaging was employed, and the data were baseline corrected to the dark response. For measurements of the light intensity, electric field, and temperature dependence of the transient PC, the transient photocurrent was amplified by a 1.1-GHz-bandwidth amplifier, and the signals from 100 laser pulses were averged. During the measurements, the light intensity was monitored by splitting part of the pulse light onto a photodiode connected to a Tektronix 468 digital storage oscilloscope.

The steady-state PC data were taken from the same samples used for the transient PC (biasing electric field of 1×10^4 V/cm) in the photon energy range between 1.38 (900 nm) and 5.0 eV (250 nm). The steady-state PC measurement was carried out using standard photomodulation techniques: the excitation light from a 150-W xenon lamp (dispersed by a grating monochromator equipped with proper order fiters) was modulated with a Stanford

SR540 mechanical chopper, and then the resulting modulated signal was processed through a computer-controlled Stanford SR530 lock-in amplifier tuned to the chopping frequency. The spectral resolution is set at about 5 nm, and the incident light intensity is about 0.3 mW/cm^2 at $\hbar\omega = 2.48$ eV (500 nm). To cancel out the spectral response of the measurement system (including the light source, grating, filters, etc.), the photoconductive cell is replaced by a calibrated photodiode and a broad-band pyroelectric detector. The spectral response of the measurement system is then taken under identical conditions and used as the background for normalization of the photoconductivity spectra.

We have characterized the MEH-PPV/C_{60} and P3OT/C_{60} films by UV-visible infrared spectroscopy and by electrical conductivity measurements (as noted earlier, the photoluminescence is quenched). Figure 1 shows the optical-absorption spectra of MEH-PPV alone, and MEH-PPV/C_{60} composite films with several concentrations of C_{60}. The absorption spectrum of C_{60} thin film[19] is also presented for comparison. The absorption data for MEH-PPV and MEH-PPV/C_{60} are normalized to unity at the peak of MEH-PPV absorption ($\hbar\omega \approx 2.5$ eV). The optical-absorption spectra of P3OT and P3OT/C_{60} films were reported previously.[2]

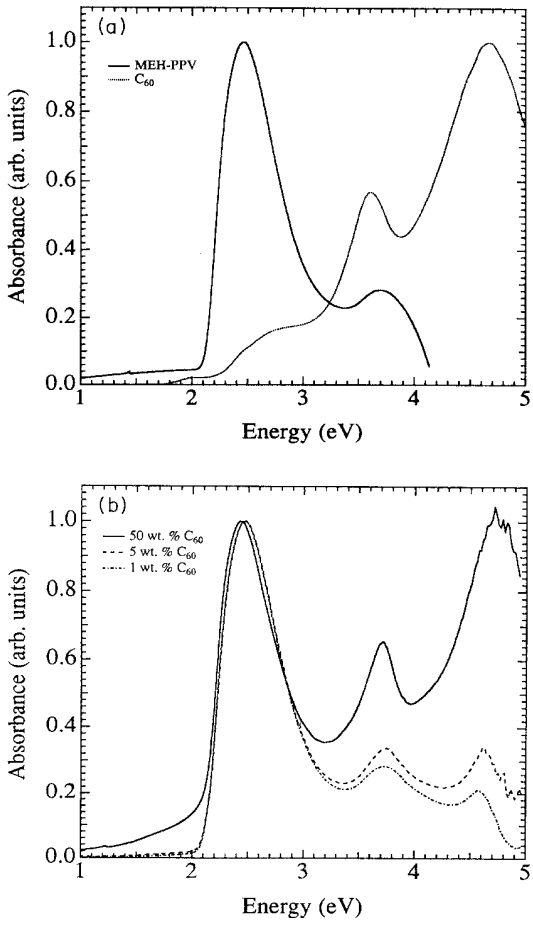

FIG. 1. (a) Optical-absorption spectra of MEH-PPV and C_{60}. (b) Optical absorption spectra of MEH-PPV/C_{60} films with several concentrations of C_{60}.

The π-π^* absorption peak of MEH-PPV is clearly observed in Fig. 1 along with the characteristic C_{60} absorption peaks (at $\hbar\omega \approx 3.6$ and 4.7 eV). Absorption spectra of MEH-PPV/ C_{60} composite films indicate that the characteristic C_{60} absorption peaks at $\hbar\omega \approx 3.6$ and 4.7 eV increase as C_{60} concentration increases. In the composites, the characteristic C_{60} absorption peaks are shifted to slightly higher energies compared with those of the pure C_{60} thin film. The weak absorption below the π-π^* gap of the conducting polymer evolves with increasing concentration of C_{60} and is mainly due to weak C_{60} absorption (symmetry forbidden in lowest order) at these energies.[20].

The absorption spectrum of the MEH-PPV/C_{60} composite film is a simple superposition of the two components without any indication of significant interaction between the two materials in the ground state. This is confirmed by measurements of the electrical conductivity; the dark conductivity of the MEH-PPV/C_{60} complex is almost identical to that of the pure MEH-PPV: $\sigma_d \approx 10^{-10} \sim 10^{9}$ S/cm. Thus the MEH-PPV/C_{60} composite forms a neutral electron *D-A* complex in which mixing of the electronic wave functions in the ground state is negligible.

For P3OT, however, there are significant changes in the absorption spectrum when C_{60} is added.[2] Although Morita, Zakhidov, and Yoshino[8] argued that these spectral changes were indicative of doping by C_{60}, subsequent studies have shown that this is not the case.[2] For example, whereas the electrical conductivity of P3OT is known to be extremely sensitive to the dopant concentration (increasing by many orders of magnitude after oxidation by a few percent of iodine or $FeCl_3$),[15] the dark conductivity of the P3OT/C_{60} complex is almost identical to that of the pure P3OT: $\sigma_d \approx 5 \times 10^{-7}$ S/cm. The changes in the absorption spectrum[2,8] indicate significant mixing of the P3OT and C_{60} electronic wave functions, and the formation of a Mulliken[21] charge-transfer complex.

III. PHOTOCONDUCTIVITY RESULTS AND DISCUSSION

A. Transient photoconductivity

Figure 2 displays the time-resolved transient photocurrent of the MEH-PPV/C_{60} composite films and a MEH-PPV film on a semilog plot. The transient PC data were taken at room temperature under a biasing electric field of 1×10^4 V/cm and normalized to an incident photon flux of 7.5×10^{14} photon/cm^2 per pulse at $\hbar\omega = 2.92$ eV. The rise time (less than 100 ps) is limited by the temporal resolution of the detecting system. In the 50 wt % composite, a transient photovoltaic signal, i.e., photoresponse under the zero bias) is observed; this was subtracted from the transient PC wave form. Due to the poor photoconductive response of the pristine MEH-PPV (and the resulting time resolution), the initial decay of the transient PC signal is not resolved; however, experience

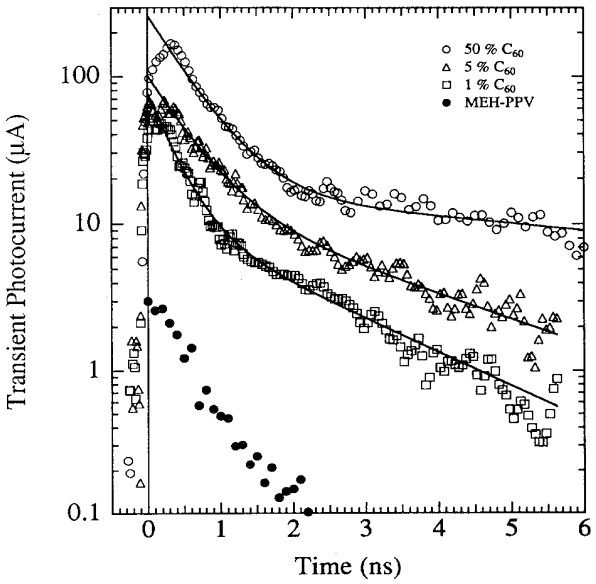

FIG. 2. Wave forms of the time-resolved transient photocurrent in MEH-PPV/C_{60} films and a MEH-PPV film at room temperature on a semilog plot. The PC data for MEH-PPV/C_{60} are taken at $\hbar\omega=2.92$ eV with a time resolution of about 50 ps, whereas the MEH-PPV data are taken at $\hbar\omega=3.7$ eV with a sampling gatewidth of 2 ns. The transient PC data were normalized to an incident photon flux of $\approx 7.5\times 10^{14}$ photons/cm^2 per pulse. The solid lines are fits of the transient PC decay of MEH-PPV/C_{60} to the double exponential form Eq. (1). The fitting parameters are summarized in Table I.

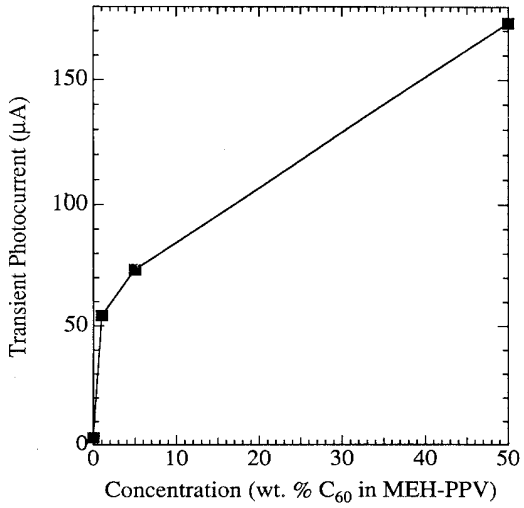

FIG. 3. The dependence of the transient PC on the C_{60} concentration; the magnitude of the transient PC peaks at room temperature, shown in Fig. 2, are plotted vs C_{60} concentration (by wt %) in MEH-PPV.

with other conjugated polymers suggests an initial fast decay (a few hundred ps).[17,18,22]

The solid lines in Fig. 2 represent best fits to the transient PC decay of the MEH-PPV/C_{60} composites assuming the double exponential form

$$I_{\rm ph}(t)=A\exp(-t/\tau_1)+B\exp(-t/\tau_2)\ . \qquad (1)$$

The fitting parameters and their dependence on the C_{60} concentration are summarized in Table I. The extension of the longer lifetime (τ_2) by addition of C_{60} is much more dramatic than that of the initial fast decay time (τ_1).

The magnitude of the transient photoconductivity of pristine MEH-PPV is relatively small. Using the N_2 laser ($\hbar\omega=3.7$ eV) with a flux for photoexcitation of $\approx 6\times 10^{15}$ photons/cm^2 per pulse, we found the peak transient photoconductivity in MEH-PPV to be $\sigma_{\rm ph}\approx 2\times 10^{-3}$ S/cm.

Compared to pristine MEH-PPV, both the magnitude and lifetime of the transient PC are enhanced with increasing concentration of C_{60} in the MEH-PPV/C_{60} films. The magnitude of the transient PC (peak values) is plotted in Fig. 3 versus C_{60} concentration (wt %) in MEH-PPV; the initial PC increases sharply at low concentrations and then more slowly at higher concentra-

TABLE I. The fitting parameters to the transient PC decay of the MEH-PPV/C_{60} composites using the double exponential form $I_{\rm ph}(t)=A\exp(-t/\tau_1)+B\exp(-t/\tau_2)$.

Concentration	A (μA)	τ_1 (ps)	B (μA)	τ_2 (ns)
1 wt % C_{60}	66.0	320	11.5	1.86
5 wt % C_{60}	85.0	498	16.4	2.52
50 wt % C_{60}	247.3	523	16.6	9.89

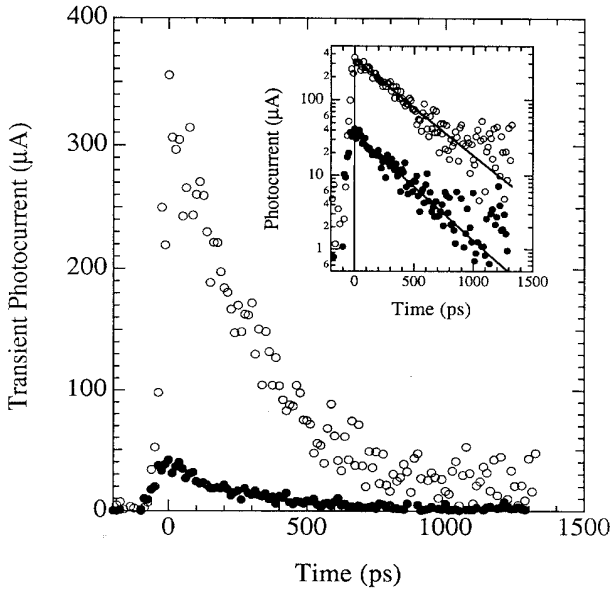

FIG. 4. Wave forms of the time-resolved subnanosecond transient PC in P3OT/C_{60} (open circles) and P3OT (solid circles) at room temperature, upon photoexcitation at $\hbar\omega=2.92$ eV under a biasing electric field of 2×10^4 V/cm. The transient PC data were normalized to an incident photon flux of $\approx 3\times 10^{15}$ photons/cm^2 per pulse. In the inset the same data are plotted on a semilog plot, and the solid lines are single exponential fits to the PC data.

tions. With an addition of 1% C_{60} the PC is enhanced by a factor of 20 to a value comparable with that of pure C_{60}.[19]

The results shown in Fig. 3 are qualitatively consistent with photoinduced electron transfer: recombination is inhibited by the spatial separation of the electron and hole on the C_{60} and the conducting polymer, respectively. This same effect is responsible for the increase in τ_2 as the concentration of C_{60} is increased (see Fig. 2 and Table I).

Figure 4 displays wave forms of the time-resolved subnanosecond transient photocurrent in a P3OT/C_{60} film and a P3OT film, upon photoexcitation at $\hbar\omega=2.92$ eV under a biasing electric field of 2×10^4 V/cm. The transient PC data were normalized to an incident photon flux of approximately 3×10^{15} photons/cm^2 per pulse. Each wave form shows that the transient PC peak is followed by a rapid decay which can fit to an exponential dependence, as shown by the semilog plot in the inset. The transient PC in P3OT/C_{60} (5 wt %C_{60}) is nearly an order of magnitude larger than in P3OT with a slightly increased carrier lifetime ($\tau\approx350$ ps compared to $\tau\approx300$ ps for P3OT). The magnitude of the transient PC in P3OT/C_{60} increases substantially (as in MEH-PPV/C_{60}), indicating photosensitization and an increase in the quantum efficiency for photogeneration of charge carriers. In P3OT/C_{60}, however, the carrier lifetime shows no significant enhancement. In particular, the long tail observed in MEH-PPV/C_{60} is not detected in the P3OT/C_{60}. We infer that C_{60} acts as a deeper trap in P3OT (once trapped, the release time for the carriers is much longer).

Although the transient PC relaxation in the MEH-PPV/C_{60} composite can be fit to the double exponential form [Eq. (1)] in the early time regime, the photocurrent decay after about 5 ns is a power law, $I_{ph}(t)\sim t^{-\alpha}$, where $\alpha\approx1.16$, as shown for the 1:1 MEH-PPV/C_{60} composite sample in the log-log plot of Fig. 5. This long-time photocurrent decay was taken at room temperature after

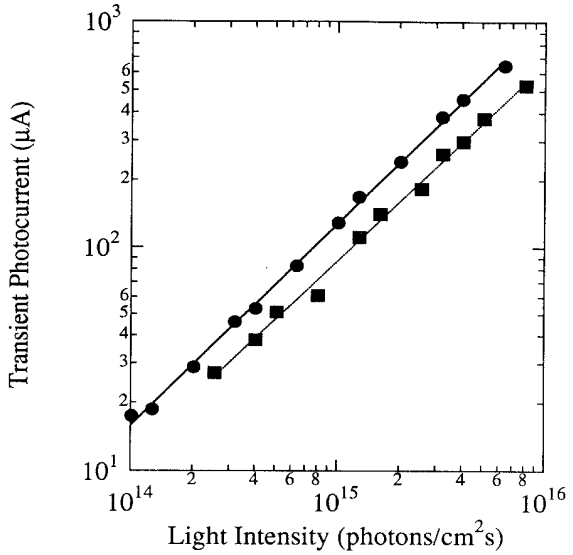

FIG. 6. The excitation light intensity dependence of the transient PC peak for the 1:1 MEH-PPV/C_{60} composite, measured at $\hbar\omega=2.58$ (solid squares) and 2.92 eV (solid circles) at room temperature.

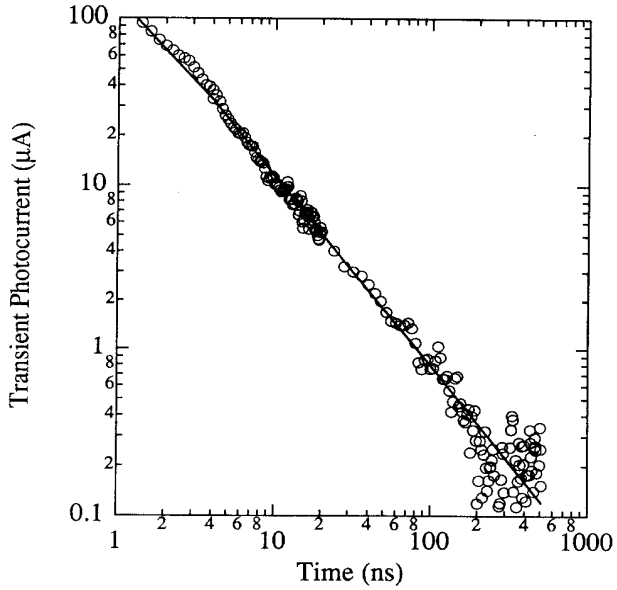

FIG. 5. The transient photocurrent decay after ≈5 ns for the 1:1 MEH-PPV/C_{60} composite sample (log-log plot). The data were taken at room temperature after photoexcitation at $\hbar\omega=2.92$ eV with an incident photon flux of about 3×10^{15} photons/cm^2 per pulse. The fitting curve shows a power-law decay $I_{ph}(t)=t^{-\alpha}$, where $\alpha\approx1.16$.

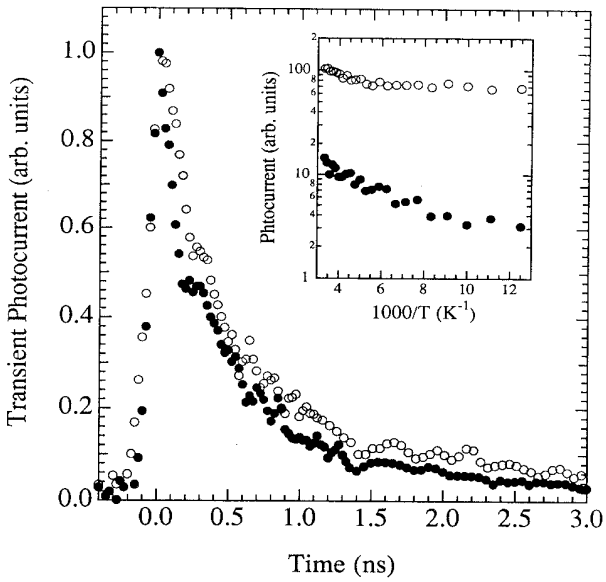

FIG. 7. The temperature dependences of the transient photocurrent in the 5 wt % MEH-PPV/C_{60} film are plotted for the sample at room temperature (open circles) and 81 K (solid circles). The wave forms were obtained with an incident flux of about 2×10^{15} photons/cm^2 per pulse at $\hbar\omega=2.92$ eV and normalized to unity at the peak. The inset shows the temperature dependence of the initial transient PC peak and the photocurrent at 2 ns after the peak.

photoexcitation at $\hbar\omega = 2.92$ eV with an incident photon flux of about 3×10^{15} photons/cm^2 per pulse. Since the photocurrent was amplified by a 1.1-GHz-bandwidth amplifier, and the sampling gatewidth is chosen to be 2 ns; the data in Fig. 5 are valid only for times greater than several nanoseconds.

Figure 6 shows the intensity dependence of the transient PC peak for the 1:1 MEH-PPV/C_{60} composite, measured at $\hbar\omega = 2.58$ (481 nm) and 2.92 eV (425 nm) at room temperature. The transient PC peak at both energies shows a quasilinear intensity dependence, approximately $I^{0.9}$.

In Fig. 7 the transient PC wave form measured at room temperature is compared with that measured at 81 K for the 5 wt % MEH-PPV/C_{60} composite. The wave forms are obtained with an incident photon flux of about 2×10^{15} photons/cm^2 per pulse at $\hbar\omega = 2.92$ eV, and normalized to unity at the peak. The inset shows the temperature dependence of the initial transient PC peak and the photocurrent at 2 ns after the peak. The fast initial photoresponse shows very weak temperature dependence; the magnitude of the transient PC peak decreases by only 30% upon cooling from 300 to 80 K. This weak temperature dependence of the subnanosecond transient PC peak has been observed in a number of conducting polymers; for example, in polyacetylene,[17] poly(3-hexylthiophene),[18] poly(*p*-phenylenevinylene),[22], and polydiacetylene.[23] The slow component, however, is thermally activated with an activation energy of $E_a \approx 18$ meV. The small activation energy, together with the power-law decay of the long tail (see Fig. 5), suggests that the transport (and recombination) of charge carriers is dominated by rather shallow traps in this ns time scale. Moreover, the more strongly activated steady-state PC (see Sec. III B) suggests that the photocarriers thermalize into deeper traps as time progresses. Therefore, the temperature independence of the subnanosecond PC response implies pretrapping transport, implying that the fast decay probably results from the initial trapping.

B. Steady-state photoconductivity

Figure 8 shows the spectral response of the steady-state PC of a pristine MEH-PPV film and MEH-PPV/C_{60} films with several concentrations of C_{60} for photon energies from 1.38 (900 nm) to 5.0 eV (250 nm). The data were taken at room temperature using a modulated light source and lock-in amplifer detection (35-Hz chopping frequency) with the sample biased at 1×10^4 V/cm. The PC data are normalized to a constant incident photon flux of about 7.5×10^{14} photons/cm^2 s.

For MEH-PPV, the photoconductive spectral response shows a sharp onset at $\hbar\omega \approx 2.0$ eV which coincides with that of the optical absorption from the π-π^* interband transition of MEH-PPV (see Fig. 1). The photoconductive response of the MEH-PPV/C_{60} composites increases sharply at about $\hbar\omega \approx 1.3$ eV, lower than that of either MEH-PPV or C_{60}. The spectral response of the photoconductivity of pure C_{60} closely follows the optical-absorption spectrum of C_{60}, with PC onset at $\hbar\omega \approx 1.6$ eV.[19] The PC data from samples sensitized with 1 and 5

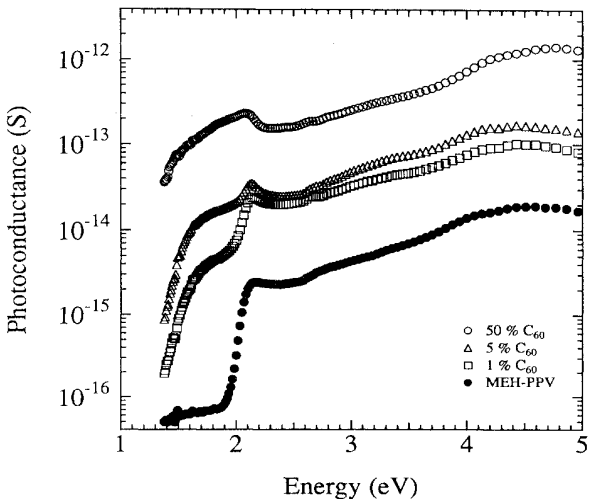

FIG. 8. Spectral response of the steady-state PC of MEH-PPV and MEH-PPV/C_{60} films with several concentrations of C_{60} at room temperature. The data were normalized to the constant incident photon flux of $\approx 7.5 \times 10^{14}$ photons/cm^2 s (mechanically chopped at 35 Hz).

wt % C_{60} show a plateau at 1.6–2.0 eV. The photoinduced absorption of the MEH-PPV/C_{60} composites has also been reported to show a sharp edge at about $\hbar\omega \approx 1.15$ eV, and a plateau at 1.6–2.0 eV, again different from the PIA spectrum of MEH-PPV.[1,2] Thus the photoinduced charge transfer in the excited state of the composites is clearly evident, even though the optical-absorption spectrum indicates no charge transfer in the ground state (see Fig. 1). The PC of MEH-PPV/C_{60} increases sharply again at the same onset energy of the π-π^* interband transition of MEH-PPV ($\hbar\omega \approx 2.0$ eV), as is clearly evident in the films sensitized with 1 and 5 wt % C_{60}. For $\hbar\omega > 2.0$ eV, the PC spectrum of the composite films is essentially identical to that of the pristine MEH-PPV, but with enhanced magnitude.

The observation that the PC response of both MEH-PPV and MEH-PPV/C_{60} increases sharply at the *same* energy ($\hbar\omega \approx 2.0$ eV) implies that photogeneration of charge carriers in MEH-PPV occurs through the π-π^* interband transition rather than dissociation of photogenerated excitons. If there were a significant exciton binding energy (E_{exc}) in MEH-PPV, energy would be required to separate the electron and the hole. Consequently, unless there were evidence of the formation of a charge-transfer complex, the enchanced transient PC response would be activated with an activation energy comparable to E_{exc}. Such activated behavior is not observed; the ultrafast photoinduced electron transfer and the resulting enhanced PC response occur at room temperature and below (see Fig. 7). On the contrary, these ultrafast photoinduced electron transfer results can be readily understood within a band model of the electronic structure of the PPV derivative.[22]

The composite films exhibit the expected enhanced PC

response over the entire spectral range from the near infrared to the ultraviolet. The enhancement of the PC response due to sensitization by C_{60} is particularly clear at photon energies below the π-π^* interband transition of MEH-PPV, since at these photon energies the absorption is mainly due to absorption by the C_{60}. Although we observe substantially enhanced steady-state PC, it is impossible to distinguish from the steady-state PC alone whether the observed sensitization is due to enhanced quantum efficiency or to enhanced carrier lifetime (or both), since the steady-state PC is proportional to their product. The time-resolved transient PC data clearly demonstrate, however, the incorporation of C_{60} enhances *both* the quantum efficiency and the carrier lifetime. Note that the significant effect of C_{60} on the charge-carrier generation efficiency can be inferred independently from the steady-state PC, by the observation that incorporation of even 1 wt % C_{60} in MEH-PPV (i.e., far below the percolation threshold) enhances the steady-state PC by more than an order of magnitude.

Figure 9 shows the spectral response of the steady-state PC of a pristine P3OT film and a P3OT/C_{60} film (5 wt % C_{60}) at room temperature. The data are taken under the same experimental conditions as in Fig. 8. The photoconductive spectral response in both P3OT and P3OT/C_{60} shows a sharp onset at $\hbar\omega \approx 1.9$ eV from the π-π^* interband transition of P3OT. For P3OT/C_{60}, a weak photoconductive signal due to absorption by C_{60} is observed below the π-π^* interband transition of P3OT. The peak at $\hbar\omega \approx 3.7$ in the PC action spectrum for P3OT/C_{60} (not detected for the P3OT spectrum) might also result from the C_{60} absorption peak at this energy. As in the MEH-PPV/C_{60} composities, the enhancement of the PC response due to sensitization by C_{60} is clearly evident over the entire spectral range.

The magnitudes of the photoconductivity in the sensitized films are given in the photoconductance spectra, for MEH-PPV/C_{60} in Fig. 8 and for P3OT/C_{60} in Fig. 9. Although the incorporation of C_{60} in MEH-PPV and P3OT significantly enhances the photoconductivity over the values obtained in the pristine materials, the magnitude of the photocurrent is still relatively small.

Figure 10 shows the temperature dependence of the dark conductivity and the steady-state PC of the 1:1 MEH-PPV/C_{60} composite. The dark conductivity shows Arrhenius behavior with a thermal activation energy of $E_a \approx 70$ meV in the temperature range from 300 to 100 K, and a slightly lower activiation energy below 100 K. The steady-state PC shows much stronger temperature dependence than the dark conductivity; the activation energy of the steady-state PC is $E_a \approx 220$ meV for $\hbar\omega < 2.0$ eV, and $E_a \approx 180$ meV for $\hbar\omega > 2.0$ eV at $T > 200$ K. At lower temperatures, $T < 200$ K, $E_a \approx 80$ meV for $\hbar\omega < 2.0$ eV, and $E_a \approx 60$ meV for $\hbar\omega > 2.0$ eV. The larger activation energy for the photoexcitation at $\hbar\omega < 2.0$ eV suggests a more localized nature for the states in the π-π^* gap of MEH-PPV.

Figure 11 shows the dependence of the steady-state PC on the excitation light intensity for the MEH-PPV/C_{60} composites and MEH-PPV, measured at $\hbar\omega = 3.1$ eV (400 nm) at room temperature. The light intensity was changed by using neutral density filters. The steady-state PC of MEH-PPV/C_{60} exhibits the same intensity dependence as that of MEH-PPV; the fits to the data indicate a slightly sublinear power-law dependence, approximately $I^{0.8}$. A similar sublinear intensity dependence was obtained over all spectral ranges in all samples (although the 50 wt % sample shows a somewhat more sublinear intensity dependence, approximately $I^{0.7}$, at high photon energy). We also found a slightly superlinear electric-field dependence (approximately $E^{1\sim1.5}$) of the steady-state PC in all samples, possibly arising from charging

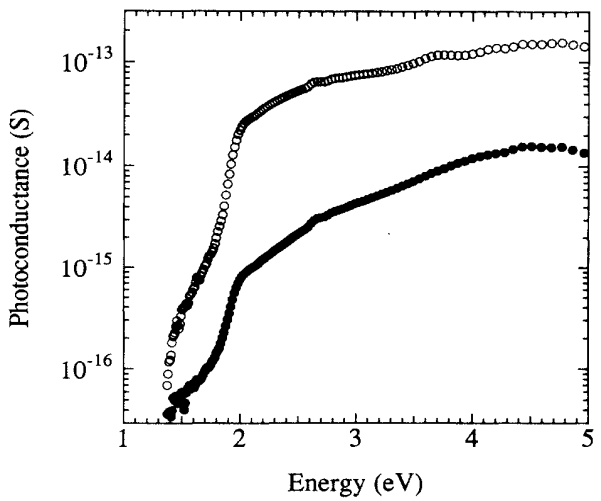

FIG. 9. Spectral response of the steady-state PC of a pristine P3OT film (solid circles) and a 5 wt % P3OT/C_{60} film (open circles) at room temperature. The data were taken under the same experimental conditions as in Fig. 8.

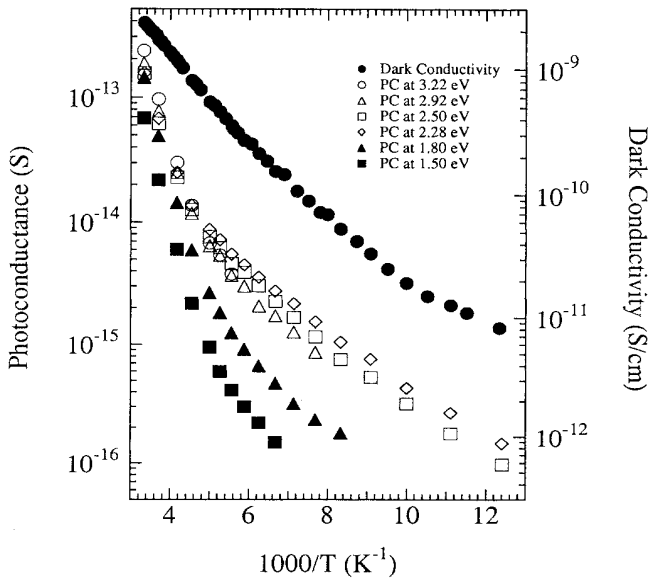

FIG. 10. The temperature dependence of the dark conductivity and the steady-state photoconductance of the 1:1 MEH-PPV/C_{60} composite sample.

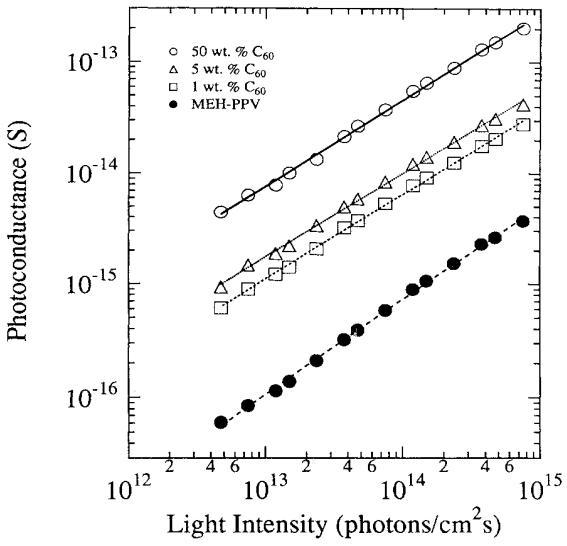

FIG. 11. The dependence of the steady-state PC on the excitation light intensity at room temperature for MEH-PPV/C_{60} and MEH-PPV, measured at $\hbar\omega = 3.1$ eV (400 nm).

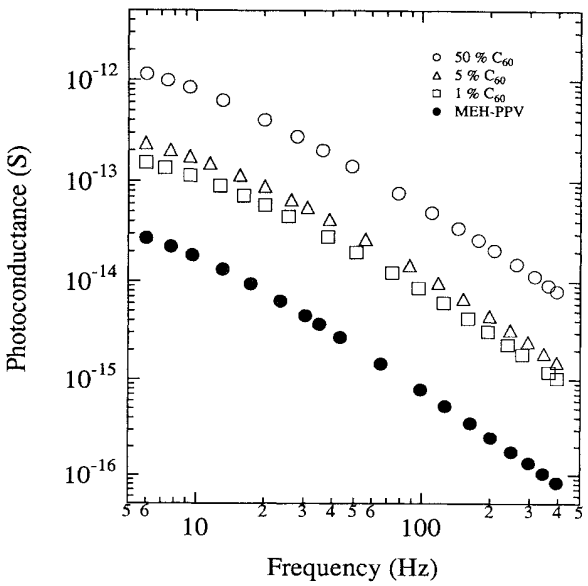

FIG. 12. The dependence of the steady-state PC at $\hbar\omega = 3.1$ eV on the chopping frequency at room temperature.

effects due to trapping, non-Ohmic contacts, etc.[24]

Figure 12 shows the dependence of the steady-state PC on chopping frequency for the MEH-PPV/C_{60} composites and MEH-PPV, measured at $\hbar\omega = 3.1$ eV at room temperature. As in the intensity dependence, the relaxation behavior of the MEH-PPV/C_{60} composites is similar to that of the pristine MEH-PPV. As expected from the sublinear intensity dependence, the frequency dependence of the PC cannot be fit to the expression for monomolecular recombination with a single decay rate. At chopping frequencies above about 20 Hz, the modulated PC response decreases as approximately $\omega^{-1.3}$. The power-law dependence on the chopping frequency has been understood as arising from a distribution of photocarrier lifetimes; the C_{60} molecules acting as electron traps are randomly distributed in the polymer matrix.

The power-law decay of the long-time transient PC in the MEH-PPV/C_{60} (see Fig. 5) is characteristic of dispersive transport, as expected in disordered systems,[25] and consistent with the power-law frequency dependence of the steady-state PC. The thermally activated behavior of the steady-state PC and the power-law decay of the long-time transient PC suggest trap-dominated transport at long times. The random distribution of C_{60} (electron acceptor) in the MEH-PPV matrix forms localized electronic states below the mobility edge. Since localized states act as traps, charge-carrier transport is realized via a sequence of multiple-trapping and release steps among localized states (and between localized states and extended band states) in the presence of an applied electric field. Thus the motion of a charge carrier can be viewed as a continuous-time random walk, and the resulting photocurrent follows a power-law time dependence.[24]

The similarities between the steady-state PC for MEH-PPV/C_{60} and that for MEH-PPV in the spectral shape at $\hbar\omega > 2.0$ eV (see Fig. 8), intensity dependence (see Fig. 11), and frequency dependence (see Fig. 12) indicate that carrier generation originates from photoexcitation of the MEH-PPV donor followed by electron transfer to the C_{60} acceptor, consistent with the observed correlation of the excitation profile of PIA bands in the composites with the π-π^* excitation of MEH-PPV.[1,2] We conclude, therefore, that transport of charge carriers occurs primarily in the MEH-PPV matrix; the C_{60} sensitizes the PC response by inducing electron transfer and thereby increasing the photogeneration efficiency and the charge-carrier lifetime.

IV. CONCLUSION

Transient photoconductivity in MEH-PPV/C_{60} and P3OT/C_{60} composites indicates that both the quantum efficiency for photogeneration of charge carriers and the lifetime of the carriers are increased substantially with increasing concentration of C_{60}. The results are consistent with expectations based upon the earlier observation of ultrafast photoinduced electron transfer from the conducting polymer (electron donor) to C_{60} (acceptor);[1-3] the photogeneration of charge carriers is facilitated by electron transfer in the excited state.

This sensitization of conducting polymers by C_{60} is effective because the electron transfer rate is ultrafast ($< 10^{12}$ s^{-1}); fast enough to be competitive with mechanism(s) for early time recombination (geminate and/or nongeminate) of photoexcited electrons and holes in the conducting polymer. The enhancement of the photoconductivity is observed to be greater in MEH-PPV/C_{60} than in P3OT/C_{60}, implying that the probability of early time recombination is higher in pristine MEH-PPV. Moreover, the lifetime of the transient photoconductivity is extended by the addition of C_{60}, since

recombination is inhibited by the spatial separation of the electron and hole (on the C_{60} acceptor and on the conducting polymer donor, respectively). The improved quantum efficiency and the extended carrier lifetime in the conducting polymer C_{60} composites results in significantly enhanced steady-state photoconductivity over the entire spectral range from the near infrared to the ultraviolet.

ACKNOWLEDGMENTS

This research was supported by the National Science Foundation under Grant No. NSF-DMR90-12808. We thank C. Gettinger and A. Hays for providing the purified P3OT and P3OT/C_{60} mixture solution used in these experiments.

[1]N. S. Sariciftci, L. Smilowitz, A. J. Heeger, and F. Wudl, Science **258**, 1474 (1992).

[2]L. Smilowitz, N. S. Sariciftci, R. Wu, C. Gettinger, A. J. Heeger, and F. Wudl, Phys. Rev. B **47**, 13 835 (1993).

[3]B. Kraabel, C. H. Lee, D. McBranch, D. Moses, N. S. Sariciftci, and A. J. Heeger, Chem. Phys. Lett. (to be published).

[4]N. S. Sariciftci, D. Braun, C. Zhang, V. I. Srdanov, A. J. Heeger, G. Stucky, and F. Wudl, Appl. Phys. Lett. **62**, 585 (1993).

[5]B. Miller, J. M. Rosamilia, G. Dabbagh, R. Tycko, R. C. Haddon, A. J. Miller, W. Wilson, D. W. Murphy, and A. F. Hebard, J. Am. Chem. Soc. **113**, 6291 (1991).

[6]R. C. Haddon, A. F. Hebard, M. J. Rosseinsky, D. W. Murphy, S. J. Dulcos, K. B. Lyons, B. Miller, J. M. Rosamilia, R. M. Fleming, A. R. Kortan, S. H. Glarum, A. V. Makhija, A. J. Miller, R. H. Eick, S. M. Zahurak, R. Tycko, G. Dabbagh, and F. A. Thiel, Nature **350**, 320 (1991).

[7]A. F. Hebard, M. J. Rosseinsky, R. C. Haddon, D. W. Murphy, S. H. Glarum, T. N. Palstra, A. P. Ramirez, and A. R. Kortan, Nature **350**, 600 (1991).

[8]S. Morita, A. A. Zakhidov, and K. Yoshino, Solid State Commun. **82**, 249 (1992).

[9]P. M. Allemand, A. Koch, F. Wudl, Y. Rubin, F. Diederich, M. M. Alvarez, S. J. Anz, and R. L. Whetten, J. Am. Chem. Soc. **113**, 1050 (1991).

[10]*Handbook of Conducting Polymers,* edited by T. A. Skotheim (Marcel Dekker, New York, 1986).

[11]A. J. Heeger, S. Kivelson, J. R. Schrieffer, and W. P, Su, Rev. Mod. Phys. **60**, 781 (1988).

[12]*Conjugated Polymeric Materials: Opportunities in Electronics, Optoelectronics and Molecular Electronics,* edited by J. L. Bredas and R. R. Chance (Kluwer Academic, Dordrecht, 1990).

[13]*Science and Application of Conducting Polymers,* edited by W. R. Salaneck, D. T. Clark, and E. J. Samuelsen (Hilger, Bristol, 1991).

[14]F. Wudl, P. M. Allemand, G. Srdanov, Z. Ni, and D. McBranch, in *Materials for Nonlinear Optics: Chemical Perspectives,* edited by S. R. Marder, J. E. Sohn, and G. D. Stucky (American Chemical Society, Washington, D.C., 1991), p. 683.

[15]J. Moulton and P. Smith, Synth. Met. **40**, 13 (1991); Polymer **33**, 2340 (1992).

[16]D. H. Auston, in *Picosecond Optoelectric Devices,* edited by C. H. Lee (Academic, New York, 1984), Chap. 4.

[17]M. Sinclair, D. Moses, and A. J. Heeger, Solid State Commun. **59**, 343 (1986).

[18]G. Yu, S. D. Phillips, H. Tomozawa, and A. J. Heeger, Phys. Rev. B **42**, 3004 (1990).

[19]C. H. Lee, G. Yu, D. Moses, V. I. Srdanov, X. Wei, and Z. V. Vardeny, Phys Rev. B **48**, 8506 (1993).

[20]A. Skumanich, Chem. Phys. Lett. **182**, 486 (1991); J. P. Hare, H. W. Kroto, and R. Taylor, *ibid.* **177**, 394 (1991).

[21]R. S. Mulliken, J. Am. Chem. Soc. **74**, 811 (1952).

[22]C. H. Lee, G. Yu, D. Moses, and A. J. Heeger (unpublished).

[23]D. Moses, M. Sinclair, and A. J. Heeger, Phys. Rev. Lett. **58**, 2710 (1987).

[24]A. Rose, *Concepts in Photoconductivity and Allied Problems* (Interscience, New York, 1963).

[25]H. Scher and E. W. Montroll, Phys. Rev. B **12**, 2455 (1975).